MicroRNA-133b targets TGFβ receptor I to inhibit TGF-β-induced epithelial-to-mesenchymal transition and metastasis by suppressing the TGF-β/SMAD pathway in breast cancer

SHENGJIE WANG[1,2], MINGLIANG HUANG[3], ZICHEN WANG[3], WAN WANG[3], ZHIYUAN ZHANG[3], SHUTING QU[3] and CHUN LIU[1,3]

[1]Laboratory Animal Center of Nantong University, Nantong, Jiangsu 226000; [2]Kangda College of Nanjing Medical University, Lianyungang, Jiangsu 222000; [3]Medical College of Nantong University, Nantong, Jiangsu 226000, P.R. China

Received June 13, 2019; Accepted September 4, 2019

DOI: 10.3892/ijo.2019.4879

Abstract. Breast cancer (BC) is one of the most common types of cancer and the leading cause of cancer-associated mortality among women worldwide. Accumulating evidence indicates that microRNA (miR)-133b inhibits the proliferation and invasion of cancer cells. Considering that transforming growth factor (TGF)-β signaling plays a key role in cellular epithelial-to-mesenchymal transition (EMT) and cancer metastasis, it is crucial to explore the roles and underlying molecular mechanisms of miR-133b in regulating TGF-β-induced EMT during progression of BC. In the present study, an inverse correlation was observed between the expression of miR-133b and TGFβ receptor I (TGFβR1) mRNA in BC cells and tissues. Furthermore, miR-133b expression was found to be decreased in the BC tissues of patients with lymph node metastasis and advanced tumor-node-metastasis stage, while the expression of TGFβR1 was upregulated. Overexpression of miR-133b significantly decreased the expression of TGFβR1, an indispensable receptor of TGF-β/SMAD signaling, and suppressed TGF-β-induced EMT and BC cell invasion *in vitro*, whereas miR-133b knockdown exerted the opposite effects. Mechanistically, TGFβR1 was verified as a direct target of miR-133b as determined by bioinformatics analysis and a dual-luciferase reporter assay. In addition, small interfering RNA-mediated knockdown of TGFβR1 mimicked the phenotype of miR-133b overexpression in BC cells. Furthermore, miR-133b overexpression suppressed BC cell invasion *in vivo*. Collectively, the findings of the present study indicated that miR-133b acts as a tumor suppressor, inhibiting TGF-β-induced EMT and metastasis by directly targeting TGFβR1, and suppressing the TGF-β/SMAD pathway. Therefore, miR-133b may be of value as a diagnostic biomarker of BC.

Correspondence to: Dr Chun Liu, Laboratory Animal Center of Nantong University, 19 Qixiu Road, Nantong, Jiangsu 226000, P.R. China
E-mail: liuchun@ntu.edu.cn

Key words: microRNA-133b, transforming growth factor-β receptor I, transforming growth factor-β/SMAD pathway, breast cancer, epithelial-to-mesenchymal transition, metastasis

Introduction

Breast cancer (BC) is the most frequently diagnosed cancer and the second leading cause of cancer-associated mortality among women worldwide (1). It was estimated that there were ~2.1 million newly diagnosed BC cases among women worldwide in 2018 (2). Despite significant improvements in early diagnosis and therapeutic strategies, patients with BC have a poor prognosis (3), which is predominantly due to tumor metastasis (4). Therefore, understanding the mechanisms underlying BC metastasis is crucial for developing novel therapeutic strategies for BC.

Epithelial-to-mesenchymal transition (EMT), as a vital process for tumor metastasis, is essential for the transformation of early tumors into aggressive malignancies (5). During EMT, the cells lose their epithelial characteristics, including cell polarity and specialized cell-cell adhesions, and exhibit migratory and invasive behavior (6). During the process of EMT, the expression levels of the epithelial marker E-cadherin are significantly downregulated, while those of mesenchymal cell markers, such as Snai1 and N-cadherin, are upregulated (7-9). Accumulating evidence has demonstrated that the transforming growth factor (TGF)-β/SMAD signaling pathway plays a key role in EMT (10,11). TGF-β/SMAD signaling is initiated by the binding of the TGF-β1/2 to the TGF-β receptor (TGFβR) II. The ligand-receptor complex then recruits TGFβR1 to activate downstream SMAD2/3. Phosphorylated (p-)SMAD2/3 further forms trimers with SMAD4, which translocate to the nucleus, subsequently leading to the activation of crucial transcription factors regulating EMT (12). Of note, previous studies have indicated that numerous microRNAs (miRNAs/miRs) play pivotal roles in TGF-β/SMAD signaling-mediated EMT and tumor metastasis (13-15).

miRs are a class of endogenous, highly conserved, small non-coding RNAs that are ~22 nucleotides in length, and negatively regulate gene expression by binding to the 3'-untranslated region (UTR) of target mRNAs, suppressing translation and inducing mRNA degradation (16-18). Recent studies demonstrated that miR-133b mainly acts as a tumor suppressor in numerous types of human cancer (19-21). In colorectal cancer, it has been reported that patients with low levels of miR-133b expression have a poor prognosis in terms of overall survival and positive lymph node metastasis (22). Overexpression of miR-133b inhibits the clonogenicity and invasion of BC cells (23); however, whether miR-133b affects TGF-β-induced EMT and metastasis of BC cells and the underlying mechanism remain unknown.

The aim of the present study was to investigate the association of miR-133b expression with BC metastasis and clinical stage, as well as the correlation between the expression of miR-133b and TGFβR1 in BC, hoping that the findings will provide further insight into the mechanisms by which miRNA regulates TGF-β-induced EMT and BC metastasis, and to determine whether miR-133b may be considered as a potential prognostic predictor and therapeutic target for the clinical diagnosis and treatment of BC.

Materials and methods

Patients and tissue samples. A total of 78 paired BC and adjacent normal tissues (≥2 cm away from the edge of cancer tissue, with no cancer cells identified via microscopy) were obtained from The First Affiliated Hospital of Nantong University between June 2013 and December 2018. Among the 78 patients enrolled, 42 had BC (mean age 60.9 years; range, 32-77 years), while 36 had metastatic BC (mean age, 66.3 years; range, 48-87 years). Pathological analysis of patients with BC was performed according to the Revised International System for Staging Breast Cancer (24). None of the patients had been treated with chemotherapy, radiotherapy, or any other therapy, prior to surgical intervention. All tissues were immediately frozen in liquid nitrogen following surgery, and were then stored at -80˚C until use.

Cell lines and cell culture. The human BC cell line MDA-MB-468 and the immortalized normal breast epithelial cell line MCF-10A were purchased from the American Type Culture Collection. BC cells MCF-7, MDA-MB-231 and MDA-MB-453 were obtained from the Cell Bank of Chinese Academy of Sciences. MDA-MB-231, MDA-MB-453 and MDA-MB-468 cells were cultured in RPMI-1640 medium (Gibco; Thermo Fisher Scientific, Inc.) supplemented with 10% fetal bovine serum (HyClone; GE Healthcare Life Sciences). MCF-7 cells were cultured in Dulbecco's Modified Eagle's medium (Gibco; Thermo Fisher Scientific, Inc.) with 10 μg/ml human recombinant insulin (Sigma-Aldrich; Merck KGaA) and 10% fetal bovine serum (HyClone; GE Healthcare Life Sciences). MCF-10A cells were cultured in RPMI-1640 medium with 10% fetal bovine serum and 100 ng/ml cholera toxin (Sigma-Aldrich; Merck KGaA). Cells were cultured at 37˚C in a humidified atmosphere containing 5% CO_2.

RNA extraction, cDNA synthesis, and reverse transcription-quantitative polymerase chain reaction (RT-qPCR) analysis. Cells ($2x10^6$) and tissues (200 mg) were employed for total RNA extraction using TRIzol® reagent (Thermo Fisher Scientific, Inc.), according to the manufacturer's protocols. The concentration and purity of total RNA were detected using a NanoDrop2000 spectrophotometer (NanoDrop Technologies; Thermo Fisher Scientific, Inc.). Pre-designed stem-loop RT primers were employed to synthesize the cDNA of miR-133b and U6 (25), and random primers were used for the cDNA synthesis of TGFβR1. The synthesis of cDNA using reverse transcriptase was performed using the M-MLV First Strand kit (Thermo Fisher Scientific, Inc.), according to the manufacturer's protocol. Briefly, the reaction conditions were as follows: 25˚C for 10 min, 42˚C for 45 min, and 85˚C for 5 min. qPCR was performed using SYBR Green qPCR SuperMix-UDG kits (Thermo Fisher Scientific, Inc.) according to the manufacturer's instructions. The thermocycling conditions were as follows: Initial preincubation at 95˚C for 10 min, followed by 40 cycles of amplification at 95˚C for 5 sec and at 60˚C for 30 sec. qPCR was performed on an ABI Prism 7500 Real-Time PCR system (Applied Biosystems; Thermo Fisher Scientific, Inc.). The primer sequences used for RT and qPCR were pre-synthesized (Genewiz Inc.) and are summarized in Table I. U6 was used for the normalization of miR-133b expression, whereas β-actin served as an endogenous control for TGFβR1 mRNA expression. RT-qPCR analysis was conducted in triplicate; relative expression levels were evaluated using the $2^{-\Delta\Delta Cq}$ method (26).

Establishment of stable cell lines overexpressing miR-133b. To stably overexpress miR-133b (LV-miR-133b) in MDA-MB-231 cells, the miR-133b sequence was cloned into the pLKO.1-puro vector (InovoGen Tech. Co.) via the *Age*I and *Eco*RI (Fermentas; Thermo Fisher Scientific, Inc.) sites to generate the pLKO.1-puro miR-133b plasmid. Then, the aforementioned construct or control vector with the packaging plasmids psPAX2 and pMD2.G (Geneseed Biotech) were co-transfected into 293T cells to produce the lentivirus. MDA-MB-231 cells were infected with the lentivirus and selected with 1 μg/ml puromycin (Sigma-Aldrich; Merck KGaA) to obtain stable cell lines (LV-miR-133b). Finally, the stable cell lines were used for *in vivo* experiments of metastasis. The sequence of the miR-133b segment was 5'-CCGGUC AGAAGAAAGAUGCCCCCUGCUCUGGCUGGUCAAACG GAACCAAGUCCGUCUUCCUGAGAGGUUUGGUCCCCU UCAACCAGCUACAGCAGGGCUGGCAAUGCCCAGUCC UUGGAGA-3'.

RNA oligonucleotides and cell transfection. In the present study, two small interfering (si)RNAs) were employed, which were designed using BLOCK-iT™ RNAi Designer (https://rnaidesigner.thermofisher.com/rnaiexpress/design.do) and synthesized by Shanghai GenePharma Co., Ltd., to specifically target TGFβR1 (si-TGFβR1-1 and si-TGFβR1-2). Scramble siRNA (si-NC) was used as a negative control. miR-133b mimic, inhibitor (anti-miR-133b) and negative controls (NCs) were obtained from Shanghai GenePharma Co., Ltd. MCF-7 and MDA-MB-231 cells were cultured on 6-well plates and transiently transfected using Lipofectamine® 3000 (Invitrogen; Thermo Fisher Scientific, Inc.) when 70-80% confluence was attained, according to the

Table I. Primer sequences for RT and RT-qPCR.

Name	Sequence (5'–3')
RT primers	
U6	CGAGCACAGAATCGCTTCACGAATTTGCGTGTCAT
miR-940	GTCGTATCCAGTGCAGGGTCCGAGGTATTCGCACTGGATACGATAGCTGGTCGTA
RT-qPCR primers	
U6	F: CGAGCACAGAATCGCTTCA; R: CTCGCTTCGGCAGCACATAT
miR-940	F: CAGTGCAGGGTCCGAGGTAT; R: CGTCTTTGGTCCCCTTCAAC
TGFβR1	F: GAGGAAAGTGGCGGGGAG; R: CCAACCAGAGCTGAGTCCAAGTA
β-actin	F: CACAGAGCCTCGCCTTTGCC; R: CATGCCGGAGCCGTTGTCG

F, forward; R, reverse; RT, reverse transcription; qPCR, quantitative polymerase chain reaction.

manufacturer's protocols. At 48 h post-transfection, the cells were harvested for further analysis. The sequences were as follows: si-TGFβR1-1, 5'-CCAUUGAUAUUGCUCCAAA-3' (sense), si-TGFβR1-2, 5'-GCAGCUAGGCUUACAGCAU-3' (sense), si-NC, 5'-UUCUCCGAACGUGUCACGU-3' (sense); miR-133b mimics, 5'-UUUGGUCCCCUUCAACCAGCUA-3' (sense), and 5'-GCUGGUUGAAGGGGACCAAAUU-3' (antisense); miR-133b NC (miR-NC), 5'-UUCUCCGAACGUGUCACGU-3' (sense), and 5'-ACGUGACACGUUCGGAGAA-3' (antisense); anti-miR-133b, 5'-GCUGGUUGAAGGGGACCAAAUU-3'; inhibitor NC (anti-miR-NC), 5'-CAGUACUUUUGUGUAGUACAA-3'.

Dual-luciferase reporter assay. The bioinformatic tools TargetScan (http://www.targetscan.org) and miRPathDB (https://mpd.bioinf.uni-sb.de/mirnas.html) were used to predict whether miR-133b targets TGFβR1. The psiCHECK-2 dual-luciferase vector (Promega Corporation) was used to generate a construct containing the TGFβR1 3'-UTR fused to the 3'-end of the luciferase reporter. The wild-type (WT) fragment containing predicted miR-133b target sites (positions 2,161-2,167) and mutant (MUT) fragment were directly synthesized (Genewiz, Inc.) and respectively subcloned into the psiCHECK-2 vector to create corresponding constructs. To investigate the effects of miR-133b on luciferase activity, MCF-7 and MDA-MB-231 cells were inoculated in 24-well plates, and were then co-transfected with WT or MUT 3'-UTR luciferase reporter plasmids, and miR-133b mimics or miR-NC using Lipofectamine 3000. Following transfection for 48 h, the cells were harvested, and the relative luciferase activity was determined using a Dual-Luciferase Reporter Assay System (Promega Corporation) on a TD20/20 Luminometer (Turner Designs) according to the manufacturer's protocols. The relative luciferase activity was presented as the ratio of *Renilla*/firefly in accordance with the Dual-Luciferase Assay Manual (27). Each experiment was repeated in triplicate.

Western blot assay. Cell protein lysates were prepared using radioimmunoprecipitation assay buffer (Cell Signaling Technology, Inc.) with protease and phosphatase inhibitor cocktail (Beyotime Institute of Biotechnology), according to the manufacturers' instructions. The protein concentration was determined using a Bicinchoninic Acid Protein Assay kit (Beyotime Institute of Biotechnology) and separated by 10% SDS-PAGE. Proteins were subsequently transferred to polyvinylidene difluoride membranes (EMD Millipore). The membranes were blocked with 3% bovine serum albumin (Beyotime Institute of Biotechnology) for 2 h at room temperature, and then incubated overnight at 4˚C with primary antibodies against TGFβR1 (1:3,000; cat. no. AF3025; R&D Systems, Inc.), N-cadherin (1:3,000; cat. no. 610920; BD Biosciences), Snail (1:1,000; cat. no. 3895s; Cell Signaling Technology, Inc.), p-SMAD3 (1:3,000; cat. no. Ab52903; Abcam), SMAD3 (1:3,000; cat. no. 9523S; Cell Signaling Technology, Inc.) and β-actin (1:5,000; cat. no. af5172; Affinity) according to the manufacturer's protocols. Then, the membranes were incubated at room temperature for 1.5 h with goat anti-rabbit IgG (1:4,000; cat. no. BA1054; Beyotime Institute of Biotechnology) or goat anti-mouse IgG (1:4,000; cat. no. BA1050; Beyotime Institute of Biotechnology) secondary antibodies. The protein bands were visualized with an electrochemiluminescence kit (Vazyme) and analyzed with a ChemiDoc™ XRS system (Bio-Rad Laboratories, Inc.). Western blotting was performed in triplicate and representative images are presented.

Transwell migration and invasion assays. For the migration assay, 8-μm Transwell chambers (Corning Incorporated) were prepared, whereas the membranes of chambers coated with Matrigel (200 ng/ml; BD Biosciences) were used for the invasion experiments. According to the manufacturer's protocols, at 48 h following transfection, MCF-7 and MDA-MB-231 cells were trypsinized and counted. A total of $5x10^4$ cells in 100 μl serum-free RPMI-1640 medium were added to the upper chamber, and 600 μl RPMI-1640 medium supplemented with 20% fetal bovine serum was added to the lower chamber. After 6 h, TGF-β1 (5 ng/ml) was added to the lower chambers. After culturing for 24 h (migration) or 36 h (invasion) in a 5% CO_2 incubator at 37˚C, the upper chamber was removed, and the non-migrating or non-invading cells were wiped away using a cotton swab. The cells in the lower chamber were fixed with 100% methanol for 20 min and stained with 0.1% crystal violet solution for 1 h at room temperature. Cells in five random

fields (magnification, x100) were imaged and counted under a light microscope. Experiments were performed in triplicate.

In vivo metastasis assays. To assess lung metastasis, 5-week-old female BALB/c nude mice were purchased from the Laboratory Animal Center of Nantong University. The mice were divided into two groups (5 mice per group), including the LV-miR-133b and control (LV-miR-NC) groups. The mice were bred and housed under specific pathogen-free conditions. LV-miR-133b and LV-miR-NC MDA-MB-231 cells ($3x10^5$ cells/mouse) in PBS were injected into the tail vein of mice. At 8 weeks following the injection of MDA-MB-231 cells, the mice were euthanized; the lungs were collected and fixed in Bouin's solution for metastatic nodule analysis, or fixed with 4% polyoxymethylene for H&E staining.

H&E staining. According to the H&E staining protocols (15), the lung tissues were fixed in 4% paraformaldehyde overnight at room temperature, and dehydrated through an ethanol gradient [60, 70, 80, 95, 100 (I) and 100% (II)] for 20 min per concentration. Then, the samples were embedded in paraffin for 40 min at 60˚C and cut into 5-μm sections. The lung tissue sections were dewaxed with xylene (I) and xylene (II) for 10 min, followed by rehydration via an ethanol gradient (100, 95, 80, 70 and 60%) for 5 min per concentration. Subsequently, the tissue sections were washed with distilled water for 2 min, followed by hematoxylin staining for 5 min, and washing in distilled water for 30 sec. Subsequently, the samples were treated with 1% hydrochloric acid ethanol for 10 sec and washed for 15 min. Next, the lung tissue sections were stained with 1% eosin for 2 min and washed for 2 min. The tissue sections were dehydrated via an ethanol gradient (95, 95, 100 and 100%), and then cleared with xylene (I) and xylene (II) for 10 min. The sections were sealed with neutral gum and viewed under a light microscope (Olympus Corporation).

Statistical analysis. SPSS 23.0 (IBM Corp.) and GraphPad Prism 7.01 (GraphPad Software, Inc.) were used for all statistical analyses. In clinical samples of BC, differences between two groups were assessed using paired or unpaired Student's t-tests (two-tailed). The association between the expression levels of miR-133b or TGFβR1, and the clinicopathological parameters of patients with BC were analyzed by non-parametric tests (Mann-Whitney U test for two groups, and a Kruskal-Wallis test for multiple groups). The correlation between the miR-133b and TGFβR1 mRNA expression level ratios (T/N) in the BC tissues was analyzed by Spearman's rank correlation analysis. Differences among multiple groups were determined by one-way ANOVA followed by Tukey's post hoc test. Prognostic analysis was performed using the Kaplan-Meier method with log-rank test. The results from tissues are presented as box and whiskers with minimum and maximal values, while other data are expressed as mean ± standard deviation. All data were generated from three independent experiments. P<0.05 was considered to indicate a statistically significant difference.

Results

miR-133b expression is downregulated and is inversely associated with TGFβR1 expression in BC cells and tissues. In order to investigate the association between miR-133b and TGFβR1, RT-qPCR was performed using four human BC cell lines. As shown in Fig. 1A, miR-133b expression levels were notably decreased in the MCF-7, MDA-MB-231, MDA-MB-453 and MDA-MB-468 cell lines compared with those in the immortalized normal breast epithelial cell line MCF-10A. Additionally, the four BC cell lines exhibited significantly increased TGFβR1 mRNA expression levels (P<0.01; Fig. 1B). To further confirm whether there is an inverse association between miR-133b and TGFβR1 mRNA expression in patients with BC, and whether it affects the development of BC, RT-qPCR was performed. From the analysis of 78 BC tissues and paired non-cancerous tissues, a significant reduction in miR-133b expression (P<0.001; 61/78, 78.2%) and a significant increase in TGFβR1 mRNA expression (P<0.001; 59/78, 75.6%) were detected in BC tissues when compared with non-cancerous breast tissues (Fig. 1C and D). Furthermore, clinicopathological analysis revealed that miR-133b expression (T/N) was markedly reduced in BC tissues from patients with advanced tumor-node-metastasis (TNM) stage and lymph node metastasis compared with those with earlier TNM stage and no lymph node metastasis (P<0.05; Table II). On the contrary, the mRNA expression levels of TGFβR1 (T/N) were higher in BC tissues from patients with advanced TNM stage and lymph node metastasis compared with those with earlier TNM stage and no lymph node metastasis (P<0.05; Table II). Of note, a significant inverse correlation was observed between miR-133b expression (T/N) and TGFβR1 mRNA expression (T/N) in 78 paired tissues (r=-0.495, P<0.001; Fig. 1E). Additionally, in order to verify these findings, datasets containing the expression data of BC tissues of the Gene Expression Omnibus and The Cancer Genome Atlas (TCGA) were analyzed. Data of the GSE19536 dataset revealed that the expression of miR-133b is downregulated in BC tissues (P<0.001; Fig. 1F); TCGA (NM_004612_1_2228) indicated that TGFβR1 mRNA expression was upregulated in invasive BC (P<0.001; Fig. 1G). These results support the findings of the present study on expression, and the association between miR-133b and TGFβR1 expression in BC cells and tissues. Collectively, these results suggest an inverse association between the expression of miR-133b and TGFβR1, which indicates a potential role for miR-133b in regulating TGFβR1 expression in BC.

miR-133b suppresses TGFβR1 expression by directly targeting TGFβR1 3'-UTR in BC cells. miRs play an important role in negatively regulating gene expression by binding to the 3'-UTR of target mRNAs (16). Therefore, it was hypothesized that miR-133b suppresses TGFβR1 expression by directly binding to the 3'-UTR of TGFβR1. To verify this hypothesis, two mRNA target-predicting tools (TargetScan 7.1 and miRPathDB) were used to identify the candidate target genes of miR-133b. As expected, TGFβR1 was validated as a putative target gene of miR-133b, as the 3'-UTR of TGFβR1 was observed to contain one conserved binding site for miR-133b (Fig. 2A). To further confirm the prediction, a dual-luciferase reporter assay was conducted (Fig. 2A) to determine whether miR-133b can recognize and target the seed region in the 3'-UTR of TGFβR1. The results revealed that miR-133b significantly inhibited the luciferase activity in MCF-7 (P<0.01; Fig. 2B)

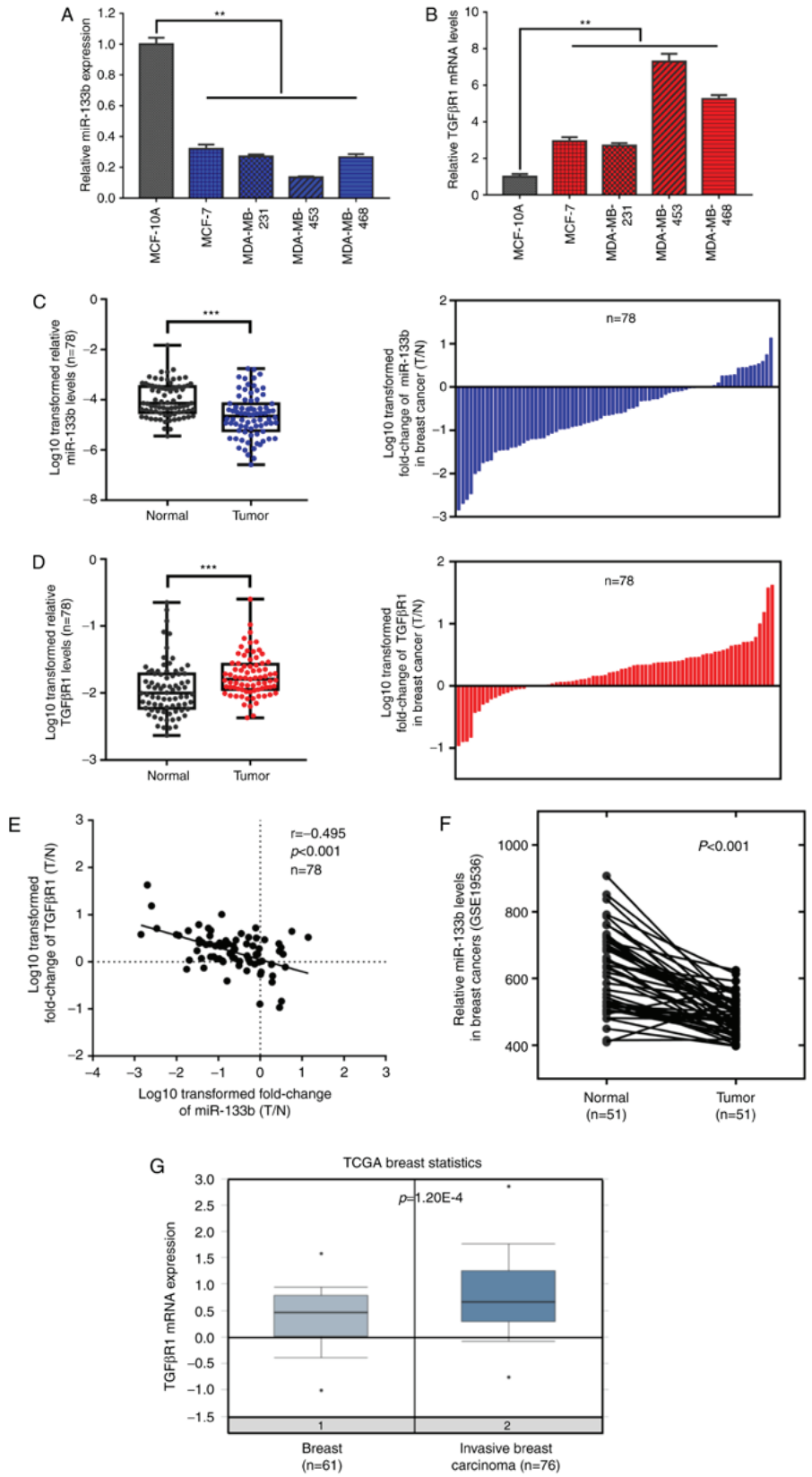

Figure 1. miR-133b expression is downregulated and inversely correlated with TGFβR1 expression in BC cell lines and tissues. RT-qPCR analysis of (A) miR-133b and (B) TGFβR1 mRNA expression levels in human breast epithelial and BC cells. U6 and β-actin were used as internal controls. Each RT-qPCR analysis was performed in triplicate. RT-qPCR analysis of (C) miR-133b and (D) TGFβR1 mRNA expression in 78 human T and N samples (left panel). Mean values are indicated by solid bars, and values are expressed as mean ± standard deviation. The log10 transformed fold change (T/N) of miR-133b and TGFβR1 expression levels of each sample are presented (right panel). U6 and β-actin were used as internal controls. (E) Correlation between miR-133b and TGFβR1 mRNA expression in 78 paired T samples. X and Y axes represent the log10 transformed fold change of T/N expression ratios of miR-133b and TGFβR1 mRNA levels, respectively. The differential expression of (F) miR-133b and (G) TGFβR1 were analyzed using the GSE19536 dataset of the Gene Expression Omnibus and The Cancer Genome Atlas (NM_004612_1_2228), respectively. Data are presented as box and whiskers with minimum and maximal values. **P<0.01, ***P<0.001. BC, breast cancer; miR, microRNA; RT-qPCR, reverse transcription-quantitative polymerase chain reaction; T, tumor tissues; N, paired non-cancerous breast tissues; TGFβR1, transforming growth factor β receptor I.

Table II. Differential expression ratios (T/N) of miR-133b and TGFβR1 mRNA between various clinicopathological parameters in breast cancer tissues.

Parameters	n	miR-133b	TGFβR1 mRNA
Age, years			
<65	38	1.044±0.383	2.220±0.403
≥65	40	0.766±0.191	2.376±0.316
[a]P-value		0.317	0.541
Pathological type			
Non-invasive carcinoma	5	1.668±0.632	2.312±0.853
Early invasive carcinoma	12	1.561±0.531	1.756±0.377
Invasive carcinoma	61	0.673±0.110	2.406±0.912
[b]P-value		0.034	0.683
TNM stage			
I	28	1.227±0.479	1.964±0.260
II	19	0.841±0.225	1.859±0.351
III and IV	31	0.460±0.141	2.874±0.543
[b]P-value		0.041	0.024
Lymph node metastasis			
No	42	1.102±0.415	1.966±0.210
Yes	36	0.729±0.162	2.689±0.486
[a]P-value		0.013	0.039

[a]Mann-Whitney U test for 2 groups. [b]Kruskal-Wallis test for 3 or more groups. The expression ratios (tumor vs. normal, T/N) of miR-133b and TGFβR1 mRNA were calculated and then analyzed according to various clinicopathological parameters. Data are presented as mean ± standard error of the mean. TGFβR1, transforming growth factor β receptor I.

and MDA-MD-231 cells (P<0.01; Fig. 2C) transfected with the TGFβR1 3'-UTR-WT reporter; however, this suppression was not observed in cells transfected with the MUT reporter (Fig. 2B and C). Additionally, overexpression of miR-133b (Fig. 2D and G) markedly decreased the expression levels of TGFβR1 mRNA (Fig. 2E and H) and protein (Fig. 2F and I) in MCF-7 and MDA-MB-231 cells, whereas cells transfected with miR-133b inhibitor (Fig. 2D and G) exhibited increased TGFβR1 expression at the mRNA (Fig. 2E and H) and protein (Fig. 2F and I) levels. In conclusion, these findings indicated that TGFβR1 is a direct target gene of miR-133b in BC cells.

miR-133b inactivates the TGF-β/SMAD pathway, and suppresses TGF-β-induced EMT and cell invasion. TGFβR1 is an important receptor of the TGF-β/SMAD signaling axis, and plays a key role in TGF-β-induced EMT and cancer metastasis (28-30). It was observed that miR-133b negatively regulates the expression of TGFβR1 (Fig. 2F and I) in BC cells. In order to determine the biological effects of decreased miR-133b expression on the progression and metastasis of BC, western blot and Transwell assays were performed to analyze the effects of miR-133b on TGF-β-induced EMT and BC cell migration and invasion. As shown in Fig. 3A and B, overexpression of miR-133b significantly inhibited the protein expression of TGFβR1 in MCF-7 and MDA-MB-231 cells. Furthermore, upon treatment with TGF-β1, BC cells transfected with miR-133b exhibited reduced expression levels of p-SMAD3, which is an indispensable downstream effector in canonical TGF-β/SMAD signaling; Snail and N-cadherin expression was reduced compared with that in miR-NC-transfected cells. Of note, the protein expression levels of SMAD3 were markedly unchanged. Conversely, the ectopic expression of miR-133b significantly suppressed the migration and invasion abilities of MCF-7 (P<0.01; Fig. 3C and D) and MDA-MB-231 (P<0.01; Fig. 3E and F) cells induced by TGF-β *in vitro*. Collectively, these results indicate that miR-133b overexpression may inhibit the expression of TGFβR1, and inhibit TGF-β1-induced EMT and cell migration and invasion via suppression of the TGF-β/SMAD signaling pathway in BC cells.

Knockdown of TGFβR1 suppresses TGF-β-induced EMT and BC cell invasion. To determine the functional role of TGFβR1, and examine whether TGFβR1 knockdown can mimic the phenotype generated by miR-133b overexpression, two siRNAs (si-TGFβR1-1 and si-TGFβR1-2) were used to specifically silence TGFβR1 expression. The results demonstrated that TGFβR1 expression was markedly downregulated in the MCF-7 and MDA-MB-231 cells transfected with TGFβR1 siRNA (Fig. 4A-C). Subsequently, the protein expression levels of EMT markers were detected in the presence or absence of TGF-β1. As shown in Fig. 4B and C, knockdown of TGFβR1 significantly inhibited TGF-β-induced upregulation of p-SMAD3, Snail and N-cadherin in MCF-7 (Fig. 4B) and MDA-MB-231 (Fig. 4C) cells. On the contrary, the protein expression levels of SMAD3 were markedly unaltered. Additionally, the results of the Transwell assays revealed that knockdown of TGFβR1 suppressed the migration (P<0.01, Fig. 4D and F) and invasion (P<0.01, Fig. 4E and G) abilities of the cells. Our results indicated that TGFβR1 knockdown mimicked the phenotype induced by miR-133b overexpression, which further suggested that miR-133b inhibits TGF-β-induced EMT, cell migration and invasion by directly targeting TGFβR1 in BC cells.

miR-133b attenuates BC cell metastasis in vivo. To further investigate the role of miR-133b overexpression in BC cell metastasis *in vivo*, LV-miR-133b MDA-MB-231 cells were established. A ~50-fold increased expression of miR-133b in LV-miR-133b MDA-MB-231 cells was observed (P<0.001; Fig. 5A). Western blot analysis confirmed the protein expression levels of TGFβR1 to be significantly downregulated in MDA-MB-231 cells stably overexpressing miR-133b compared with control cells (Fig. 5A). Then, LV-miR-133b and LV-miR-NC MDA-MB-231 cells were intravenously injected into BALB/c nude mice via the tail vein (Fig. 5B). At 8 weeks post-inoculation, the mice were euthanized and the lungs were collected for the analysis of metastases and histological examination. As expected, mice injected with LV-miR-133b MDA-MB-231 cells developed fewer metastatic nodules in the lungs (Fig. 5C and D). Consistently, H&E staining of the lungs demonstrated that the number and size of micrometastases were markedly deceased in LV-miR-133b mice compared with control mice (Fig. 5C and E). In addition, Kaplan-Meier survival analysis (31) revealed that

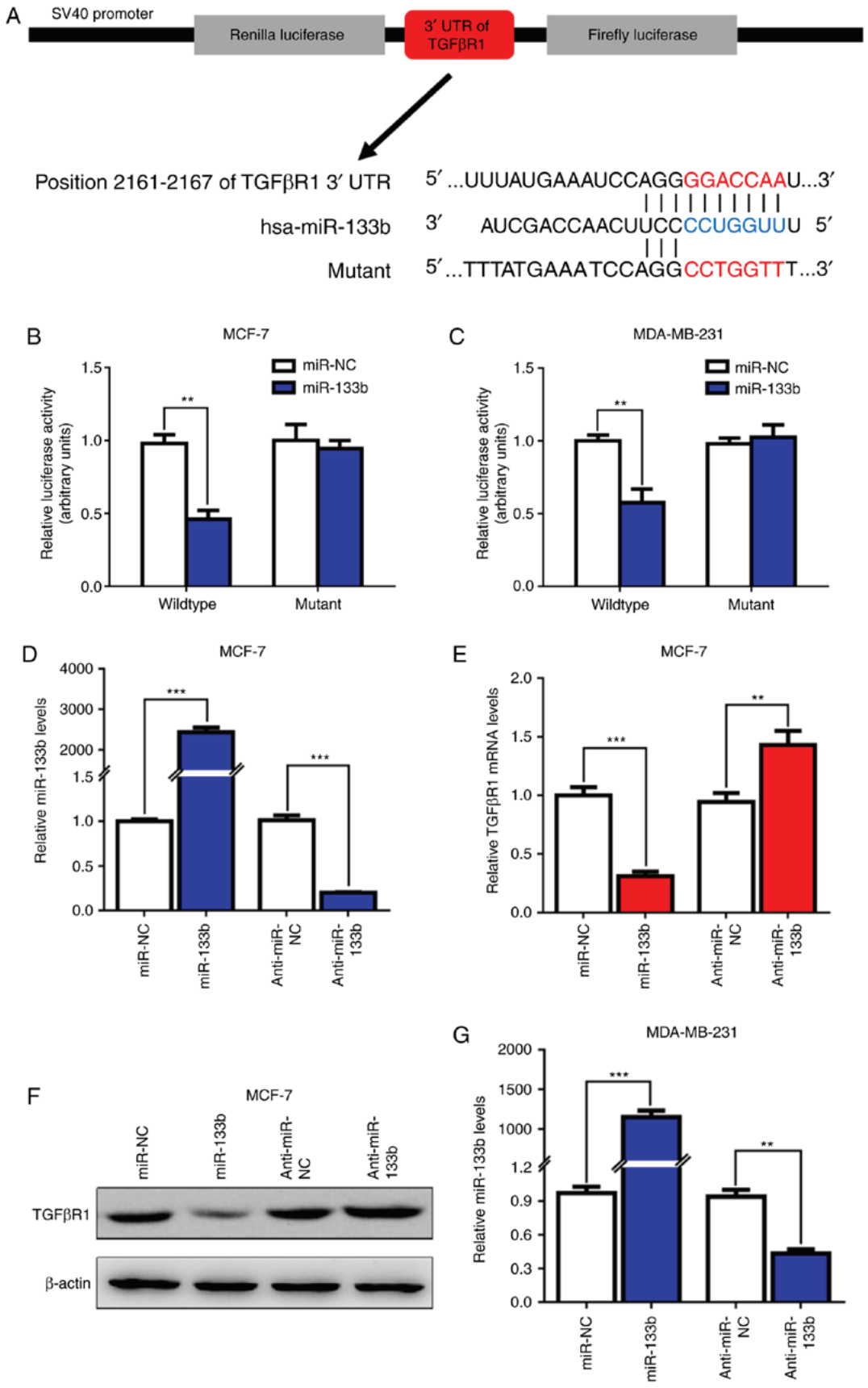

Figure 2. miR-133b inhibits TGFβR1 expression by targeting the 3'-UTR of TGFβR1 in breast cancer cells. (A) Schematic of the subcloning performed of the predicted miR-133b binding sites of TGFβR1 3'-UTR into the psiCHECK-2 luciferase vector. Predicted duplex formation between miR-133b and the wild-type/mutant of miR-133b binding sites were presented. (B and C) Relative luciferase activities of the wild-type or mutant TGFβR1 3'-UTR reporter gene in MCF-7 and MDA-MB-231 cells transfected with miR-NC or miR-133b. Relative *Renilla* luciferase activity was calculated after normalizing to firefly luciferase activity. (D) The expression levels of miR-133b were detected by RT-qPCR in MCF-7 cells after transfection with miR-133b mimics or inhibitor for 48 h. Then, the expression levels of TGFβR1 (E) mRNA and (F) protein were detected by RT-qPCR and western blotting, respectively. (G) The expression levels of miR-133b were detected by RT-qPCR in MDA-MB-231 cells after transfection with miR-133b mimics or inhibitor for 48 h. **P<0.01, ***P<0.001.

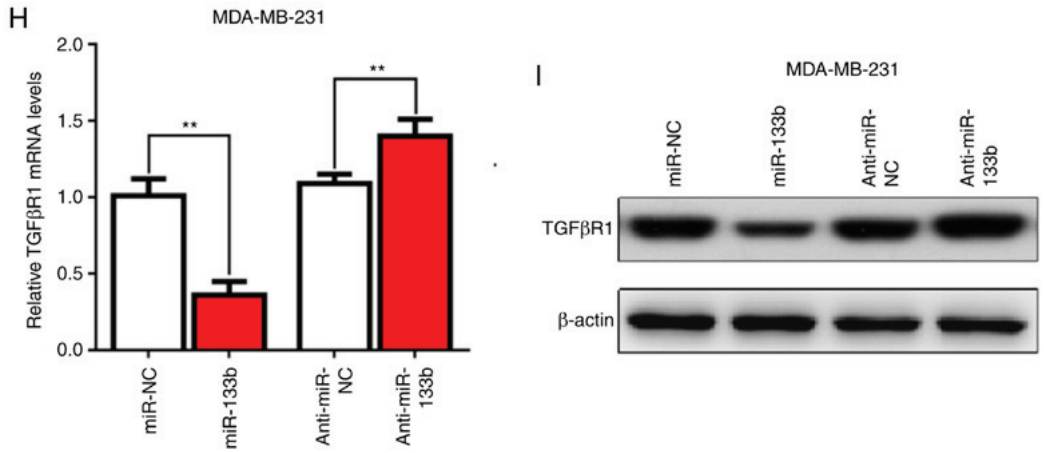

Figure 2. Continued. miR-133b inhibits TGFβR1 expression by targeting the 3'-UTR of TGFβR1 in breast cancer cells. Then, the expression levels of TGFβR1 (H) mRNA and (I) protein were detected by RT-qPCR and western blotting, respectively. **P<0.01, ***P<0.001. miR, microRNA; NC, negative control; RT-qPCR, reverse transcription-quantitative polymerase chain reaction; TGFβR1, transforming growth factor β receptor I; 3'-UTR, 3'-untranslated region.

patients with BC and low levels of miR-133b expression had significantly shorter overall survival compared with those with high miR-133b expression levels (Fig. 5F). Conversely, the expression levels of TGFβR1 were negatively associated with overall survival in patients with BC (Fig. 5G). Based on these findings, it may be concluded that low expression levels of miR-133b and high expression levels of TGFβR1 may be associated with poor prognosis in patients with BC. Collectively, these data indicate that the ectopic expression of miR-133b is associated with downregulated TGFβR1 expression, which may suppress the invasion and metastasis of BC cells *in vivo*.

Discussion

Despite advances in clinical therapy, metastasis remains the leading cause of mortality among patients with BC (32). It has been well documented that the TGF-β/SMAD signaling pathway plays an important role in EMT and tumor metastasis. Furthermore, the crucial upstream receptor of the TGF-β/SMAD pathway, TGFβR1, plays a pivotal role in TGF-β-induced EMT and tumor metastasis (28-30). miR-133b was recently reported to be involved in the development and progression of BC (23). The effects of the crosstalk between miR-133b and the TGF-β/SMAD pathway on tumor metastasis and the underlying mechanisms remain unclear, particularly in BC. To the best of our knowledge, the present study is the first to demonstrate that miR-133b directly targets TGFβR1 to inhibit TGF-β-induced EMT and metastasis via suppression of TGF-β/SMAD signaling.

Accumulating evidence has demonstrated that miRNAs play a pivotal regulatory role in the initiation and development of various cancers (33). Therefore, an in-depth understanding of the biological function of specific miRNAs in cancer may aid with the evaluation of potential therapeutic targets. Recently, dysregulated miR-133b was reported to be involved in the initiation and progression of BC (23,34); however, the effects of miR-133b on TGF-β-induced EMT and tumor metastasis and the underlying mechanisms require further investigation, particularly in BC. The aim of the present study was to investigate the biological behavior of miR-133b and the possible mechanism of action in BC. As demonstrated by the findings, miR-133b expression was found to be downregulated in BC cell lines and tissues; this decrease was significantly associated with poor prognosis of patients with BC. Furthermore, the expression of miR-133b was inversely associated with lymph node metastasis and TNM stage in patients with BC. Functional analysis indicated that miR-133b significantly inhibited TGF-β-induced EMT and BC cell invasion *in vitro* and *in vivo*. The findings of the clinical analysis revealed that miR-133b may serve as a prognostic marker in BC patients; however, whether miR-133b expression levels are correlated with BC recurrence and whether they may serve as a predictor of clinical outcome in BC is yet to be determined. Consistent with our findings, recent studies have suggested that miR-133b is also downregulated in gastric, lung and colorectal cancer (35-37). On the contrary, Qin *et al* (38) reported that miR-133b acted as an oncogene, promoting the progression of cervical carcinoma. This discrepancy may be attributed to differences in the tumor microenvironment, tumor heterogeneity or target genes.

miRNAs may act as oncogenes or tumor-suppressor genes, which is largely dependent on their targets in a variety of human cancers (39). Bioinformatic algorithms were utilized to predict potential targets, and ultimately identified a novel miR-133b-targeted gene, TGFβR1, which is a critical receptor in the TGFβ1/SMAD signaling pathway. TGFβR1 has been confirmed to play a pivotal role in TGF-β-induced EMT and tumor metastasis (28-30). It has been well-documented that TGFβ1/SMAD signaling plays a dual role in cancer development and progression. Of note, activated TGF-β/SMAD signaling serves as a tumor suppressor in early-stage tumors, but acts as a tumor promoter in late-stage tumors (40,41). Consistently, Fukai *et al* (42) demonstrated that the expression of TGFRβ1 was downregulated in early-stage human esophageal squamous cell carcinoma; however, our results were consistent with those of a recent study by Li *et al* (43) reporting that TGFβR1 mRNA expression was upregulated in hepatocellular carcinoma, with high mRNA levels of

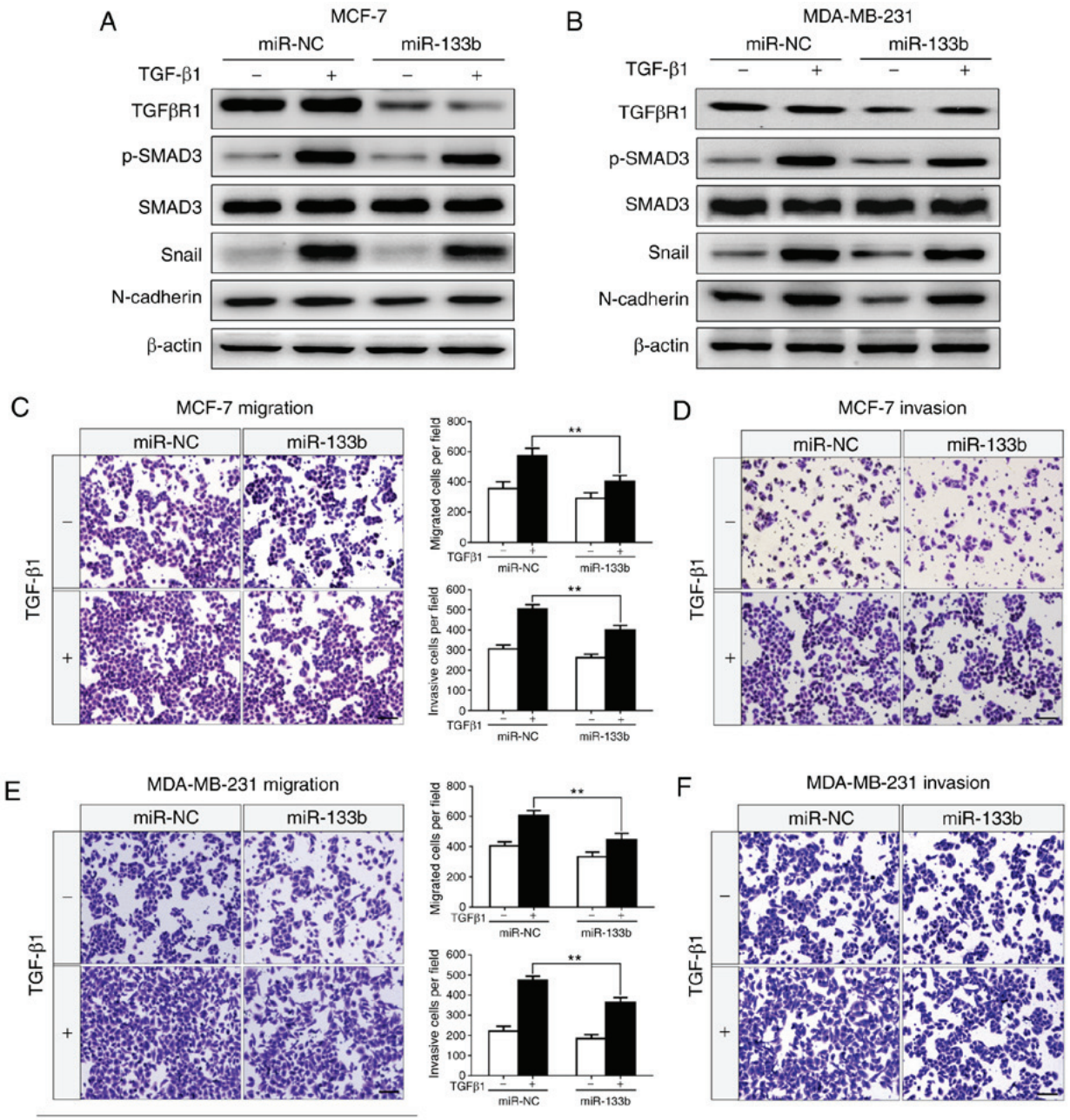

Figure 3. miR-133b suppresses TGF-β-induced epithelial-to-mesenchymal transition and invasion of breast cancer cells. (A) Western blot analysis for the expression of TGFβR1, p-SMAD3, SMAD3, Snail and N-cadherin in MCF-7 cells transfected with miR-NC or miR-133b mimics in the absence or presence of TGF-β1 (5 ng/ml) for 24 h. (B) Expression of TGFβR1, p-SMAD3, SMAD3, Snail and N-cadherin in MDA-MB-231 cells transfected with miR-NC or miR-133b mimics in the absence or presence of TGF-β1 (5 ng/ml) for 24 h. β-actin was used as an internal control. Transwell assays for MCF-7 cells transfected with miR-NC or miR-133b mimics in the absence or presence of TGF-β1 (5 ng/ml) for 24 h (migration) or 36 h (invasion). (C) Migrating and (D) invading cells were stained and counted in at least three light microscopic fields. Scale bar, 100 μm. Transwell assays for MDA-MB-231 cells transfected with miR-NC or miR-133b mimics in the absence or presence of TGF-β1 (5 ng/ml) for 24 h (migration) or 36 h (invasion). (E) Migrating and (F) invading cells were stained and counted in at least three light microscopic fields. Scale bar, 100 μm. **P<0.01. miR, microRNA; NC, negative control; TGFβR1, transforming growth factor β receptor I.

TGFβR1 being associated with advanced TNM stage (43). Furthermore, *in silico* analysis demonstrated that increased TGFβR1 expression was associated with poor prognosis of BC patients. Most importantly, we observed that siRNA-mediated knockdown of TGFβR1 suppressed TGF-β-induced EMT and BC cell invasion, whereas TGFβR1 silencing mimicked the effects and phenotype of miR-133b overexpression. The findings of the present study may provide insight into the association among miRNAs, the TGF-β/SMAD pathway and cancer metastasis. However, there were certain limitations to the present study, including insufficient materials, such as the small number of BC cell lines and BALB/c nude mice used. Moreover, the present study focused on the function of miR-133b in TGF-β-induced EMT, which is an important event promoting metastasis in advanced-stage cancers. Since TGF-β/SMAD signaling plays a key role in regulating cell proliferation in terms of cell cycle progression during the early stages of BC, it would be interesting to address the issue

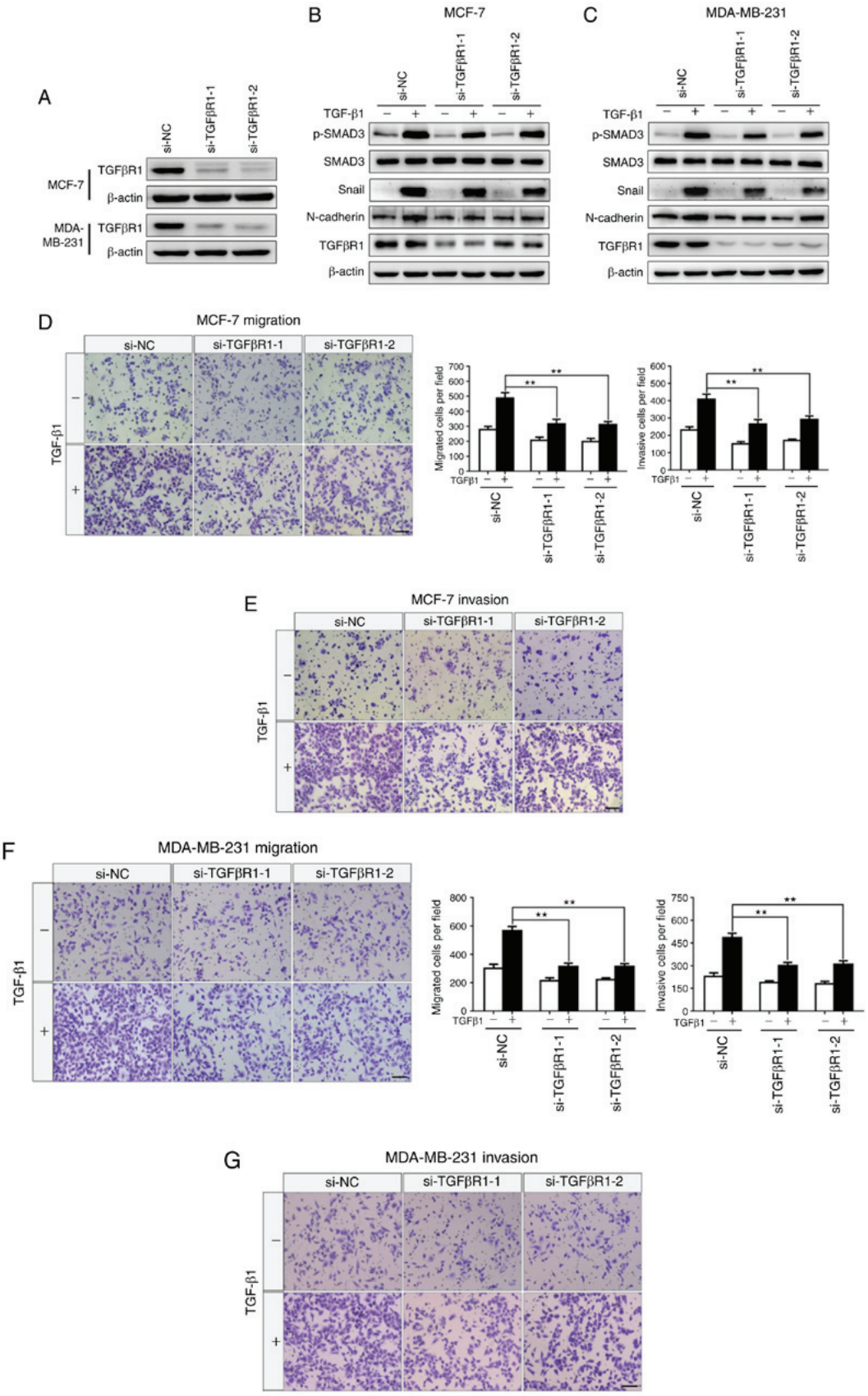

Figure 4. Knockdown of TGFβR1 suppresses TGF-β-induced epithelial-to-mesenchymal transition and invasion of breast cancer cells. (A) Western blot analysis for the expression of TGFβR1 in MCF-7 and MDA-MB-231 cells transfected with si-NC, si-TGFβR1-1 or si-TGFβR1-2. β-actin was used as an internal control. Expression of TGFβR1, p-SAMD3, SMAD3, Snail, and N-cadherin in (B) MCF-7 and (C) MDA-MB-231 cells transfected with si-NC, si-TGFβR1-1 or si-TGFβR1-2 in the absence or presence of TGF-β1 (5 ng/ml) for 24 h. Transwell assays for MCF-7 cells transfected with si-NC, si-TGFβR1-1 or si-TGFβR1-2 in the absence or presence of TGF-β1 (5 ng/ml) for 24 h (migration) or 36 h (invasion). (D) Migrating and (E) invading cells were stained and counted in at least three light microscopic fields. Scale bar, 100 μm. Transwell assays for MDA-MB-231 cells transfected with si-NC, si-TGFβR1-1 or si-TGFβR1-2 in the absence or presence of TGF-β1 (5 ng/ml) for 24 h (migration) or 36 h (invasion). (F) Migrating and (G) invading cells were stained and counted in at least three light microscopic fields. Scale bar, 100 μm. **P<0.01. siRNA, small interfering RNA; TGFβR1, transforming growth factor β receptor I.

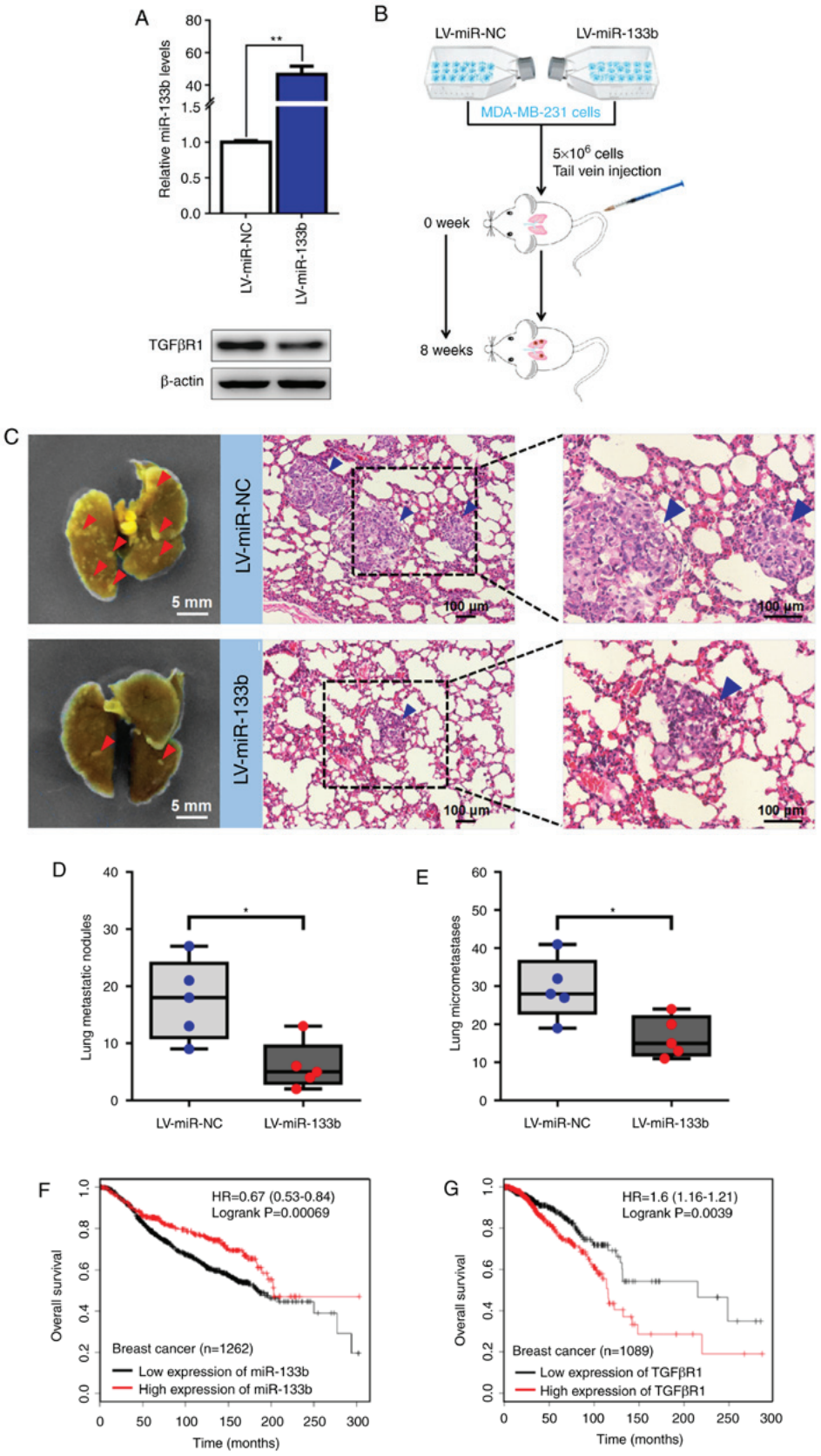

Figure 5. miR-133b attenuates BC cell metastasis *in vivo*. (A) MDA-MB-231 cells stably overexpressing miR-133b were generated. miR-133b expression was determined by reverse transcription-quantitative polymerase chain reaction analysis (upper panel). TGFβR1 expression was determined by western blot analysis (lower panel). U6 and β-actin were used as internal controls. (B) Schematic flowchart of the *in vivo* metastasis experiments with MDA-MB-231 cells, which were intravenously injected into BALB/c nude mice (n=5 mice per group). (C) Representative images of metastatic nodules in the lungs obtained from mice injected with miR-133b-overexpressing MDA-MB-231 cells or control cells (left panel). Scale bar, 5 mm. H&E staining was performed for the histological analysis of metastatic tumor cells in the lung. Scale bar, 100 μm. Red arrowheads, metastatic nodules; blue arrowheads, micrometastases. (D) Visible metastatic nodules and (E) micrometastases were counted and analyzed. *P<0.05. Survival analysis was performed using a Kaplan-Meier plotter to determine the association between the expression of (F) miR-133b and (G) TGFβR1 and the overall survival of patients with BC. **P<0.01. BC, breast cancer; LV, lentivirus; miR, microRNA; NC, negative control; TGFβR1, transforming growth factor β receptor I.

of whether miR-133b regulates the cell cycle of BC cells in future studies.

In summary, to the best of our knowledge, the present study was the first to identify that miR-133b inhibits TGF-β-induced EMT and BC metastasis via suppression of TGFβR1 expression *in vitro* and *in vivo*. These findings are further supported by the inverse association observed between miR-133b and TGFβR1 expression in BC cell lines and tissues. The results of the present study suggest a novel mechanism by which miRNA regulates TGF-β-mediated EMT and tumor metastasis, and indicate that overexpression of miR-133b may be considered as a promising strategy for treating advanced BC in the future.

Acknowledgements

Not applicable.

Funding

The present study was supported by the grants from Science and Technology Plan of Nantong (no. YYZ16044), the Students Innovation and Entrepreneurship Training Program of Nantong University (no. 2018138), the Research and Development program of Kangda College of Nanjing Medical University (no. KD2018KYJJZD002) and the '521 High-level Talent Cultivation Project' Research program of Lianyungang (no. LYG521037).

Availability of data and materials

The datasets generated and analyzed during the present study are available from the corresponding author on reasonable request.

Authors' contributions

CL and SW designed the research and analyzed the data. SW prepared the figures and drafted the manuscript. SW, MH, ZW, WW and SQ performed the experiments. All authors have read and approved the final version of this manuscript.

Ethics approval and consent to participate

The present study was approved by the Ethics Committee of The First Hospital of Nantong University (Nantong, China), and all enrolled patients provided written informed consent. The animal experiments were conducted with the approval of the Experimental Animal Ethical Committee of Nantong University, and were conducted in accordance with the Guide for the Care and Use of Laboratory Animals by US National Institutes of Health.

Patient consent for publication

Not applicable.

Competing interests

The authors declare that they have no competing interests.

References

1. Ferlay J, Colombet M, Soerjomataram I, Mathers C, Parkin DM, Piñeros M, Znaor A and Bray F: Estimating the global cancer incidence and mortality in 2018: GLOBOCAN sources and methods. Int J Cancer 144: 1941-1953, 2019.
2. Bray F, Ferlay J, Soerjomataram I, Siegel RL, Torre LA and Jemal A: Global cancer statistics 2018: GLOBOCAN estimates of incidence and mortality worldwide for 36 cancers in 185 countries. CA Cancer J Clin 68: 394-424, 2018.
3. Hartman EK and Eslick GD: The prognosis of women diagnosed with breast cancer before, during and after pregnancy: A meta-analysis. Breast Cancer Res Treat 160: 347-360, 2016.
4. Gupta GP and Massagué J: Cancer metastasis: Building a framework. Cell 127: 679-695, 2006.
5. Kang Y and Massagué J: Epithelial-mesenchymal transitions: Twist in development and metastasis. Cell 118: 277-279, 2004.
6. Xu J, Lamouille S and Derynck R: TGF-beta-induced epithelial to mesenchymal transition. Cell Res 19: 156-172, 2009.
7. Mani SA, Guo W, Liao MJ, Eaton EN, Ayyanan A, Zhou AY, Brooks M, Reinhard F, Zhang CC, Shipitsin M, *et al*: The epithelial-mesenchymal transition generates cells with properties of stem cells. Cell 133: 704-715, 2008.
8. Nieman MT, Prudoff RS, Johnson KR and Wheelock MJ: N-cadherin promotes motility in human breast cancer cells regardless of their E-cadherin expression. J Cell Biol 147: 631-644, 1999.
9. Martin TA, Goyal A, Watkins G and Jiang WG: Expression of the transcription factors snail, slug, and twist and their clinical significance in human breast cancer. Ann Surg Oncol 12: 488-496, 2005.
10. Islam SS, Mokhtari RB, El Hout Y, Azadi MA, Alauddin M, Yeger H and Farhat WA: TGF-β1 induces EMT reprogramming of porcine bladder urothelial cells into collagen producing fibroblasts-like cells in a Smad2/Smad3-dependent manner. J Cell Commun Signal 8: 39-58, 2014.
11. Divya T, Velavan B and Sudhandiran G: Regulation of Transforming Growth Foctor-β/Smad mediated epithelial-mesenchymal transition by celastrol provides protection against bleomycin-induced pulmonary fibrosis. Basic Clin Pharmacol Toxicol 123: 122-129, 2018.
12. Shi Y and Massagué J: Mechanisms of TGF-beta signaling from cell membrane to the nucleus. Cell 113: 685-700, 2003.
13. Huang G, Du MY, Zhu H, Zhang N, Lu ZW, Qian LX, Zhang W, Tian X, He X and Yin L: MiRNA-34a reversed TGF-β-induced epithelial-mesenchymal transition via suppression of SMAD4 in NPC cells. Biomed Pharmacother 106: 217-224, 2018.
14. Hu H, Xu Z, Li C, Xu C, Lei Z, Zhang HT and Zhao J: MiR-145 and miR-203 represses TGF-β-induced epithelial-mesenchymal transition and invasion by inhibiting SMAD3 in non-small cell lung cancer cells. Lung Cancer 97: 87-94, 2016.
15. Wang L, Tong X, Zhou Z, Wang S, Lei Z, Zhang T, Liu Z, Zeng Y, Li C, Zhao J, *et al*: Circular RNA hsa_circ_0008305 (circPTK2) inhibits TGF-β-induced epithelial-mesenchymal transition and metastasis by controlling TIF1γ in non-small cell lung cancer. Mol Cancer 17: 140, 2018.
16. Bartel DP: MicroRNAs: Genomics, biogenesis, mechanism, and function. Cell 116: 281-297, 2004.
17. Zamore PD and Haley B: Ribo-gnome: The big world of small RNAs. Science 309: 1519-1524, 2005.
18. Nazarov PV, Reinsbach SE, Muller A, Nicot N, Philippidou D, Vallar L and Kreis S: Interplay of microRNAs, transcription factors and target genes: Linking dynamic expression changes to function. Nucleic Acids Res 41: 2817-2831, 2013.
19. Li X, Wan X, Chen H, Yang S, Liu Y, Mo W, Meng D, Du W, Huang Y, Wu H, *et al*: Identification of miR-133b and RB1CC1 as independent predictors for biochemical recurrence and potential therapeutic targets for prostate cancer. Clin Cancer Res 20: 2312-2325, 2014.
20. Kano M, Seki N, Kikkawa N, Fujimura L, Hoshino I, Akutsu Y, Chiyomaru T, Enokida H, Nakagawa M and Matsubara H: miR-145, miR-133a and miR-133b: Tumor-suppressive miRNAs target FSCN1 in esophageal squamous cell carcinoma. Int J Cancer 127: 2804-2814, 2010.
21. Guo L, Bai H, Zou D, Hong T, Liu J, Huang J, He P, Zhou Q and He J: The role of microRNA-133b and its target gene FSCN1 in gastric cancer. J Exp Clin Cancer Res 33: 99, 2014.
22. Nohata N, Hanazawa T, Enokida H and Seki N: microRNA-1/133a and microRNA-206/133b clusters: Dysregulation and functional roles in human cancers. Oncotarget 3: 9-21, 2012.

23. Wang QY, Zhou CX, Zhan MN, Tang J, Wang CL, Ma CN, He M, Chen GQ, He JR and Zhao Q: MiR-133b targets Sox9 to control pathogenesis and metastasis of breast cancer. Cell Death Dis 9: 752, 2018.
24. Thor A: A revised staging system for breast cancer. Breast J 10 (Suppl 1): S15-S18, 2015.
25. Varkonyi-Gasic E, Wu R, Wood M, Walton EF and Hellens RP: Protocol: A highly sensitive RT-PCR method for detection and quantification of microRNAs. Plant Methods 3: 12, 2007.
26. Livak KJ and Schmittgen TD: Analysis of relative gene expression data using real-time quantitative PCR and the 2(-Delta Delta C(T)) method. Methods 25: 402-408, 2001.
27. Wolter JM, Kotagama K, Pierre-Bez AC, Firago M and Mangone M: 3'LIFE: A functional assay to detect miRNA targets in high-throughput. Nucleic Acids Res 42: e132, 2014.
28. Liu RY, Zeng Y, Lei Z, Wang L, Yang H, Liu Z, Zhao J and Zhang HT: JAK/STAT3 signaling is required for TGF-β-induced epithelial-mesenchymal transition in lung cancer cells. Int J Oncol 44: 1643-1651, 2014.
29. Fang Y, Chen Y, Yu L, Zheng C, Qi Y, Li Z, Yang Z, Zhang Y, Shi T, Luo J and Liu M: Inhibition of breast cancer metastases by a novel inhibitor of TGFβ receptor 1. J Natl Cancer Inst 105: 47-58, 2013.
30. Cortez VS, Ulland TK, Cervantes-Barragan L, Bando JK, Robinette ML, Wang Q, White AJ, Gilfillan S, Cella M and Colonna M: SMAD4 impedes the conversion of NK cells into ILC1-like cells by curtailing non-canonical TGF-β signaling. Nat Immunol 18: 995-1003, 2017.
31. Nagy Á, Lánczky A, Menyhárt O and Győrffy B: Validation of miRNA prognostic power in hepatocellular carcinoma using expression data of independent datasets. Sci Rep 8: 9227, 2018.
32. Dawood S, Broglio K, Buzdar AU, Hortobagyi GN and Giordano SH: Prognosis of women with metastatic breast cancer by HER2 status and trastuzumab treatment: An institutional-based review. J Clin Oncol 28: 92-98, 2010.
33. Nicoloso MS, Spizzo R, Shimizu M, Rossi S and Calin GA: MicroRNAs-the micro steering wheel of tumour metastases. Nat Rev Cancer 9: 293-302, 2009.
34. Chan M, Liaw CS, Ji SM, Tan HH, Wong CY, Thike AA, Tan PH, Ho GH and Lee AS: Identification of circulating microRNA signatures for breast cancer detection. Clin Cancer Res 19: 4477-4487, 2013.
35. Wen D, Li S, Ji F, Cao H, Jiang W, Zhu J and Fang X: miR-133b acts as a tumor suppressor and negatively regulates FGFR1 in gastric cancer. Tumour Biol 34: 793-803, 2013.
36. Crawford M, Batte K, Yu L, Wu X, Nuovo GJ, Marsh CB, Otterson GA and Nana-Sinkam SP: MicroRNA 133B targets pro-survival molecules MCL-1 and BCL2L2 in lung cancer. Biochem Biophys Res Commun 388: 483-489, 2009.
37. Hu G, Chen D, Li X, Yang K, Wang H and Wu W: miR-133b regulates the MET proto-oncogene and inhibits the growth of colorectal cancer cells in vitro and in vivo. Cancer Biol Ther 10: 190-197, 2010.
38. Qin W, Dong P, Ma C, Mitchelson K, Deng T, Zhang L, Sun Y, Feng X, Ding Y, Lu X, *et al*: MicroRNA-133b is a key promoter of cervical carcinoma development through the activation of the ERK and AKT1 pathways. Oncogene 31: 4067-4075, 2012.
39. Ventura A and Jacks T: MicroRNAs and cancer: Short RNAs go a long way. Cell 136: 586-591, 2009.
40. Lei Z, Xu G, Wang L, Yang H, Liu X, Zhao J and Zhang HT: MiR-142-3p represses TGF-β-induced growth inhibition through repression of TGFβR1 in non-small cell lung cancer. FASEB J 28: 2696-2704, 2014.
41. Akhurst RJ and Derynck R: TGF-beta signaling in cancer-a double-edged sword. Trends Cell Biol 11: S44-S51, 2001.
42. Fukai Y, Fukuchi M, Masuda N, Osawa H, Kato H, Nakajima T and Kuwano H: Reduced expression of transforming growth factor-beta receptors is an unfavorable prognostic factor in human esophageal squamous cell carcinoma. Int J Cancer 104: 161-166, 2003.
43. Li Y, Liu G, Li X, Dong H, Xiao W and Lu S: Long non-coding RNA SBF2-AS1 promotes hepatocellular carcinoma progression through regulation of miR-140-5p-TGFβR1 pathway. Biochem Biophys Res Commun 503: 2826-2832, 2018.